Effects of Temperature and Time on Supercritical Methanol Co-Liquefaction of Rice Straw and Linear Low-Density Polyethylene Wastes

Zhilong Yuan [a], Guangchao Jia [a], Xin Cui [a], Xueping Song [b,c,d], Cuiping Wang [e], Peitao Zhao [a,c,d*], Art J Ragauskas [c,d*]

[a] School of Electrical and Power Engineering, China University of Mining and Technology, Xuzhou 221116, PR China

[b] College of Light Industry and Food Engineering, Guangxi University, Nanning, 530004, PR China

[c] Department of Chemical and Biomolecular Engineering, University of Tennessee, Knoxville, TN, USA

[d] Joint Institute for Biological Sciences, Biosciences Division, Oak Ridge National Laboratory, Oak Ridge, TN, USA

[e] College of Civil Engineering and Architecture, Shandong University of Science and Technology, Qingdao, PR China, 266590

*Corresponding Author:

Peitao Zhao. Email: p.zhao@cumt.edu.cn, Tel/Fax: +86-516-2000

Arthur J. Ragauskas. Email: aragausk@utk.edu, Tel.: 865-974-2042, Fax: 865-974-7076

Abstract

Biofuels are particularly attractive and play an increasingly important role in sustainable energy. However, biofuels originating from lignocellulosic biomass (LCB) are extremely challenging because of their low carbon content, low stability, and high oxygen content. This work evaluates the supercritical methanol (scMeOH) co-liquefaction of rice straw and linear low-density polyethylene (LLDPE) at temperature range of 240 ~ 340 °C for 0 ~ 2 h, to obtain hydrocarbons (HCs)-rich oil and carbon-rich solid product. Results show that reaction temperature dominated the yield and properties of products, but not the holding time. Among parameters tested, 30.07 wt% oil yield with 75.79% HCs content and 33.05 wt% oil yield with 70.91% HCs content were obtained at 300 °C for 1 h and 1.5 h, respectively. Simultaneously, the remaining solid products were still as high as 53.85 wt% with a carbon content of 79.59% and 48.28 wt% with carbon content of 81.34% under 300 °C for 1 h and 1.5 h, respectively. Ultimate analysis, FT-IR, TGA, and SEM show that solid products could be used as sustainable carbon resources, and solid fuel rather than soil amendment because of risk of micro plastic or adsorbent due to smooth surface without pores.

Keywords: Rice straw, linear low-density polyethylene, supercritical methanol, co-liquefaction, hydrocarbons-rich oil

1. Introduction

The past century has witnessed the huge success of petrochemical industry, while the significant challenges associated with fossil fuel utilization with the depletion of petroleum resources, environmental crises, climate change and its adverse effects on health have motivated substantial studies on conversion of renewable and carbon-neutral

biomass energy into marketable chemicals [1-3]. Biomass consisted of forestry residues, agriculture residues, and municipal solid waste, etc. [4]. Lignocellulosic biomass (LCB), as one of the most important biomass, is abundant availability, carbon neutrality, and sustainability compared to conventional energy sources, which has the highest potential to contribute the energy needs [5]. As one of most important LCB, rice straw (RS) comprised of cellulose, hemicellulose, and lignin [6]. It has been considered as energy material to produce transportation fuels because of its high photosynthetic efficiency [7] and growth rate, and wide sources [8].

However, bio-oil directly originating from RS has typical limitations, e.g., low bio-oil yield, high oxygen content [9], and complex compositions similar to other biomass [8, 10, 11], which severely hindered its practical applications. Hence, it is necessary to upgrade the bio-oil, which was usually achieved by two common techniques: 1) catalytic upgrading [11, 12], and hydrodeoxygenation (HDO) [7], and 2) co-feeding LCB with hydrogen-rich materials e.g., sludge [13, 14] and plastic [15]. Yuan et al. [16] reported the supercritical liquefaction of RS in mixed solvent of ethanol–water and 2-propanol–water mixture, and phenols was the main composition of the bio-oil. A similar result was also observed by Li et al. [17], in which only a small amount of hydrocarbons was obtained. Cao et al. [18] studied the effect of co-solvent (glycerol and water) on bio-oil yields from RS, and reported the improvement of the bio-oil production, but not the increase of hydrocarbons content (as high as 100% oxygenates). Chen et al. [11] investigated on the catalytic hydrothermal liquefaction (HTL) of RS for bio-oil production with Ni/CeO_2 catalyst and the maximum 10.64% of hydrocarbons content in

bio-oil was achieved under the optimal Ni/CeO_2 ratio of 1/5 and the temperature of 290 °C. Huang et al. [14] studied on the co-liquefaction of sewage sludge and RS, and reported a slight improvement in bio-oil quality. Till today, few studies have addressed the subject of co-liquefaction of RS with hydrogen-rich plastics. However, this should be considered if plastic wastes can be used as a new improver for efficiently enhancing quality and quantity of RS-derived bio-oil free of catalyst.

Previous studies had reported that co-liquefying other biomasses with plastics, such as polyethylene (PE), could provide hydrogen and carbon to improve oil quality and quantity [13, 15, 19]. In addition, co-feeding with plastics could also dispose plastic wastes, which are the major source of white pollution [20, 21]. These works mentioned above had discussed the influence of adding plastic to biomass on oil production, and environmental protection. However, two issues still need to be further discussed. First, the researches on improving oil quality were very limited in chemical compositions of oil. Second, it is still unclear for the potential utilization of solid products containing plastic. The characteristics of solid products derived from co-liquefaction of feedstocks containing plastic was quite different from those produced from single biomass liquefaction [21, 22]. However, previous studies mainly focused on oil properties, and the fundamental data for solid product was very limited to elemental analysis or thermogravimetric analysis. Table S1 summarizes a detailed information on highlights and limitations from main works about liquefying RS. Therefore, the in-depth studying in co-liquefaction of LCB and plastic wastes is worth to be further investigated.

In this work, rice straw (RS) and linear low-density polyethylene (LLDPE) were

selected as materials to conduct co-liquefaction of LCB and plastic waste over a broad temperature range of 240 ~ 340 °C and holding time of 0 ~ 2 h. The yields of oil and solid products at various conditions were recorded, analyzed, and discussed. Oils was characterized by gas chromatography-mass spectrometer (GC-MS) to evaluate the oil quality, and solid products were analyzed by elemental analysis, Fourier transform infrared spectrometer (FT-IR), thermogravimetric analysis (TGA), and scanning electron microscope (SEM) to observe their elemental data, thermal stability, functional groups composition, and microstructure to explore their potential utilization.

2. Materials and methods

2.1 Materials preparation

Rice straw (RS) was collected from local farmland (Xuzhou, China) and dried in vacuum oven at 105±5 °C until no weight variation. Then it was crushed into fine particles with a size of 0.15-0.50 mm and stored in a desiccator to prevent moisture absorbing. LLDPE with a density of 0.93 g/cm^3 was obtained from Exxon Corporation, and its particle size is around 0.15-0.80 mm. Fundamental data of both feedstocks could be found in previous study [23].

2.2 Experimental setup and procedure

Supercritical methanol (scMeOH) co-liquefaction was carried out in a Parr 4590 reactor (Parr Instrument Company, USA). Fig. 1 presents the schematic diagram, experimental setup and procedures. At each run, 3 g of mixture of RS to LLDPE mass ratio of 1:2 based on optimum [23] was mixed with 30 mL (about 23 g) methanol. Reactor was initially purged with N_2 (99.999%) for 5 min to create an oxygen-free environment.

Later, the reactor was heated to the pre-determined temperature (240, 260, 280, 300, 320, and 340 °C) and maintained there for desired time (0, 0.5, 1, 1.5, and 2 h). The stir kept rotating at a speed of 65 rpm to ensure the uniform of the samples. After reaction, the reactor was naturally cooled down to ambient temperature.

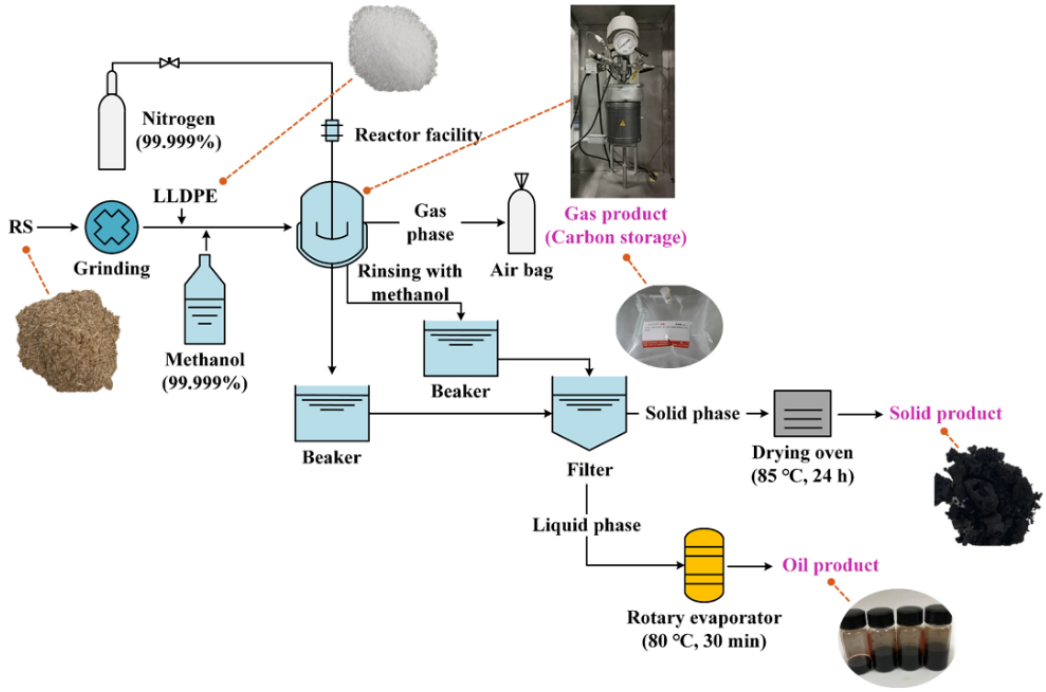

Fig. 1. Schematic diagram, experimental setup experimental procedure.

The gas products mainly dominated by carbon dioxide, similar to result from Hadhoum et al [24]. Hence, the gas products were directly vented without further analyzing after cooling. The remaining products were collected in a beaker, and the reactor was washed with methanol to recover the residuals. The slurry products were mechanically separated into two parts as solid and liquid phases. The solid residues were dried in an oven at 105±5 °C to obtain the yield of solid product. The liquid fraction was evaporated at atmospheric pressure by a rotary evaporator with a water bath at 85 °C to recover the oil.

The total yields of gas product as well as loss during collection, separation, and extraction grouped together as "gas + loss" and calculated by difference [25, 26]. The yields of oil and solid products are determined based on weight fraction of target products to pre-dried feedstocks by the following equations:

$$Yield_{oil}\,(wt\%) = \frac{W_{oil}}{W_{RS} + W_{LLDPE}} \times 100\% \quad (1)$$

$$Yield_{solid\ product}\,(wt\%) = \frac{W_{solid\ product}}{W_{RS} + W_{LLDPE}} \times 100\% \quad (2)$$

$$Yield_{gas+loss}\,(wt\%) = 100\% - yield\ of\ oil - yield\ of\ solid\ product \quad (3)$$

The conversion rate was calculated by the following equation.

$$Conversion\ rate\ (\%) = 100\% - yield\ of\ solid\ product \quad (4)$$

2.3 Products characterizing

The chemical compositions of oils were analyzed by GC-MS (Agilent 7890A/5975C-GC-MS). Tentative identification of the all compounds was performed using NIST mass spectral database (NIST11). The detailed information could be found in previous work [23].

The carbon, nitrogen, and hydrogen content of feedstocks, and solid products were tested by elemental analyzer (Vario Macro Cube*, Germany). The oxygen content was determined by difference, assuming negligible sulphur in the products:

$$O\,(wt\%) = 100 - C - H - N - Ash\,(wt\%) \quad (5)$$

The higher heating value (HHV) of solid products was determined using Dulong formula [27, 28]:

$$HHV\,(MJ/kg) = 0.3383C + 1.422\,(H - O/8) \quad (6)$$

LabsysEvo (SETARAM) was used to reveal thermal stability of solid products [29]. In each run, ~ 15 ± 3 mg of solid products was heated at 30 ~ 850 °C under heating rate of 30 K/min, under N_2 atmosphere. FT-IR spectra of solid residua was obtained by a */VERTEX 80v to show the variation of functional groups in the wavenumber range of 500 ~ 4000 cm^{-1}.

3. Results and discussion

3.1 Effects of temperature and time on products distribution

Fig. 2a depicts the products distribution from scMeOH co-liquefaction of RS/LLDPE mixture under various temperature for 1 h. The oil yield calculated by Eq. 1 was notably increased from 12.23 wt% to 30.07 wt% as temperature rose from 240 °C to 300 °C. It decreased to 22.03 wt% with further increasing temperature to 340 °C. This was due to the enhancement of gasification at higher temperature (above 300 °C). In detail, the gas formation required a relatively high activation energy than oil and solid products [13]. When reaction temperature was high enough, the reaction system would provide enough energy to convert part of oil fragments into light molecules such as gases by secondary degradation [25], thus reducing oil yield.

Accordingly, the solid yield calculated by Eq. 2 was decreased rapidly from 85.77 wt% at 240 °C to 39.03 wt% at 340 °C. This was equivalent to an increase in conversion rate by 46.74%. Apparently, solid product yield was still high at 340 °C, which could be attributed to two reasons. First, the high proportion (i.e., 66.67 wt%) of LLDPE in feedstock and stable structure of polymer with alone degradation temperature of 400 °C [30, 31] led to a limited transformation into gas or oil, and the majority of unreacted or

reformed LLDPE transferred into solid product, thus increasing the yield of solid product. Second, RS mainly consisted of cellulose, hemicellulose, and lignin. Cellulose and hemicellulose could be degraded at 240 °C and 180 °C [32, 33], respectively, whereas lignin had a high decomposition temperature of 350 ~ 400 °C [34]. Hence, degraded lignin also contributed to solid product yield.

Compared to results from RS liquefaction [11, 18, 35], no extremal point for solid product yield or conversion rate was observed at a broad temperature range (i.e., 240 ~ 340 °C) in present study. This could be ascribed to interactive reactions among intermediates or free radicals derived from the decomposition of RS and LLDPE. As mentioned previously, reformed LLDPE was major component of solid product, which would be accelerated to degrade via enhanced synergistic effect under high temperature. Detailed possible reasons could be summarized as follows: 1) the cellulose, hemicellulose components of RS were degraded by a serious of dehydration, and decarboxylation to produce esters, ketones, alcohols, etc. while lignin component was thermally decomposed into phenolic compounds [36]. These oxygenated compounds and free radicals were further decomposed and depolymerized into highly reactive and light molecular fragments under the effect of methanol free radicals of $H\bullet$, $HO\bullet$, $CH_3\bullet$ [24, 37]. Simultaneously, LLDPE was cracked by random scission and chain end scission to generate aliphatic hydrocarbons (C_xH_y) and free radicals ($C_{x-m}H_{y-n}\bullet$) with various length [20]. All these unstable fragments and intermediates from both RS and LLDPE were rearranged through polymerization, condensation, and cyclization, and gasification reactions, etc. [24] generating new organics compounds to restrict solid formation. 2) The

CH• free radicals generated by random scission and chain-end scission of LLDPE could easily catch oxygenated free radicals from RS, which would block the agglomeration and coking among the free radicals [31], restricting the formation of solid product.

Fig. 2b exhibits the effect of holding time (i.e., 0 ~ 2 h) on products distribution at 300 °C. Clearly, the holding time had a little effect on yields of oli and solid product at 300 °C. Oil yield was firstly increased from 24.51 wt% to 33.05 wt% with holding time lengthening from 0 h to 1.5 h. It was slightly declined to 31.04 wt% as holding time prolonging to 2 h. This is because part of oil products was further degraded to gaseous product [25]. For solid yield, it continuously decreased to 48.03 wt% by 6.98 wt% as time increased from 0 h to 2 h. Compared to the effect of reaction temperature, it could be concluded that adjusting reaction temperature was more efficient for improving products distribution instead of time. Besides, 300 °C for 1.5 h was determined preliminarily as an optimum condition because of its highest oil yield of 33.02 wt%. The highest oil yield of 26.00 wt% was obtained at 280 °C for 30 min without catalyst by Singh et al. [35]. The difference in the oil yield was reasonable considering a number of internal factors, e.g., reactor, solvents, and complexities of RS characteristic from different origin, even the country. With the help of Na_2CO_3, Cao et al. [18] obtained the greatest oil yield of around 68.00wt% under 15 g of RS, 150 mL of glycerol, and 0.75 g under 260 °C. Similarly, Chen et al. [11] used Ni/CeO_2 (2/10) as catalyst and yielded a maximum oil of 65.60wt% under temperature of 290 °C for 1h and pressure of 2.00 MPa, and holding time of 1 h from RS. Obviously, catalyst promoted the decomposition of feedstock resulting in higher oil production.

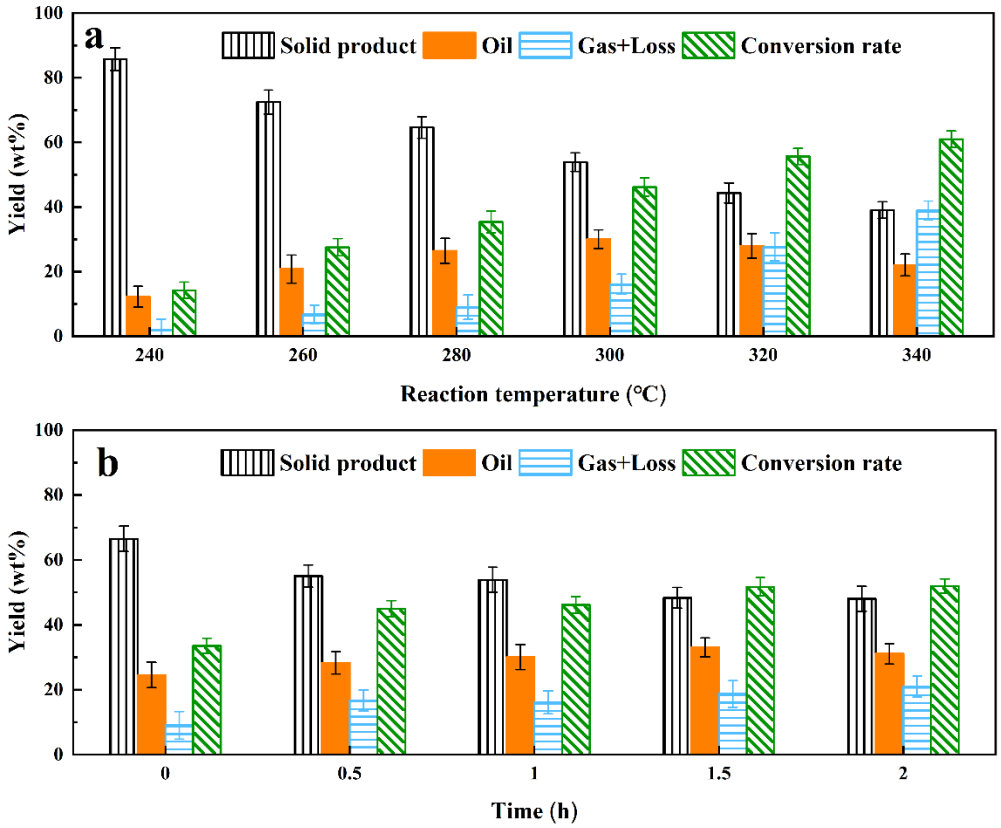

Fig. 2. Effect of temperature and time on products distribution from scMeOH co-liquefaction of RS and LLDPE under a) various temperature (i.e., 240 ~ 340 °C) for 1 h, and b) different time (0 ~ 2 h) at 300 °C.

3.2 Effecs of temperature and time on oil properties

Fig. 3a shows the GC-MS spectra of oils under various temperature (240 ~ 340 °C) for 1 h. Generally, increasing temperature could result in much lighter molecules in oils [38]. However, the main GC-MS peaks of oils did not shift towards light molecular weight with an increase of temperature from 240 °C to 340 °C. By contrast, an irregular m/z distribution of compounds in oil was observed. This result reveals that the complex interactive reactions between the intermediates of RS and LLDPE existed in co-liquefaction. There was a little difference in GC-MS spectra of oils generated by varying holding time at 300 °C, with an exception of 0 h (Fig. 3b), indicating that reaction temperature was a crucial factor in controlling chemical compositions of oil and interplay effect between RS and LLDPE. Table S2 and Table S3 exhibit the detailed information

of compounds identified by GC-MS spectra from different temperature and time. Oils were composed of a variety of organic compounds, which were categorized into 3 groups as hydrocarbons (C_xH_y), nitrogen compounds ($C_xH_yO_zN_m$), and oxygenates ($C_xH_yO_z$) e.g., ester, ketones, and phenols. The compound with more than one functional group were named as diverse functional group compounds (DFGCs) according to NIST mass spectral database (NIST11), such as propionic acid, 2-isopropoxy-, methyl ester of oil from 240 °C for 1 h consisted of –O- and –COO- groups), and 2-furamethanol of oil from 300 °C for 0 h was composed of –OH and –O– groups.

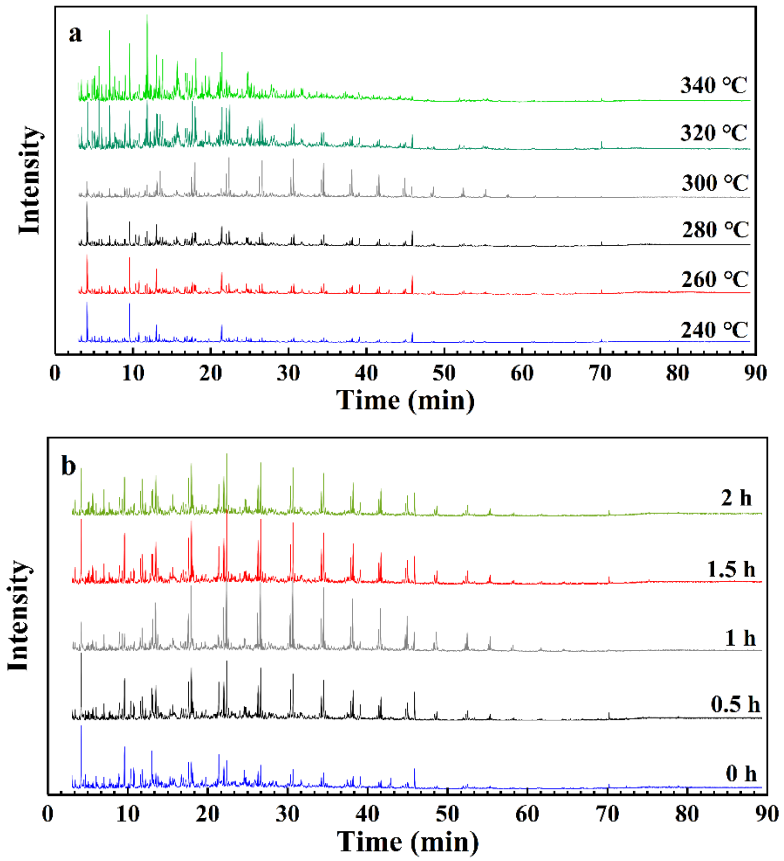

Fig. 3. GC-MS chromatograms for oils produced by a) varying reaction temperature (i.e., 240 ~ 340 °C) for 1 h and b) holding time (i.e., 0 ~ 2 h) at 300 °C.

Fig. 4a depicts the effect of temperature on chemical compositions of oil under constant time 1 h. As shown, yield of the hydrocarbons (HCs) in oils was firstly increased from 11% at 240 °C to its maximum with 75.79% at 300 °C, and then reduced sharply to

2.42% at 340 °C. As discussed previously, increasing temperature (from 240 °C to 340 °C) resulted in more LLDPE to degrade. Generally, the deep degradation of LLDPE could result in more hydrocarbons and their intermediates. However, HCs yield in oil did not increase at high temperature ranges (300 °C above), which were only 33.90 and 2.42% at 320 and 340 °C, respectively. The reason could be attributed to the promotion of lignin degradation by synergistic effect between RS and LLDPE [31]. It has been confirmed that polyolefins could readily donate hydrogen to biomass radicals in pyrolytic conditions (i.e., absence of H_2O) [39]. LLDPE could be solubilized by the biomass-derived intermediates ($C_{x-m}H_{y-n}O_{z-l}\bullet$), and then it was degraded into monomeric or oligomeric fragments. These fragments were further reacted with reactive biomass decomposition products [20]. In detail, lignin was an aromatic polymer structure, and consisted of phenylpropane units connected by both C-O-C and C-C bonds [40]. These bonds were more difficult than the glycoside bonds to break [41]. At high temperature range, the C-C bonds in lignin structure would be attacked by $CH_2\bullet$ radicals originated from LLDPE degradation to generate more oxygenates instead of hydrocarbons [42]. Therefore, hydrocarbons content in oil was reduced at 320 °C, and 340 °C. This result suggests that production of hydrocarbons (HCs)-rich oils from scMeOH co-liquefaction of RS and LLDPE strongly depended on reaction temperature. In others words, interactions between RS and LLDPE could be selectively conducted towards producing HC-rich oils by controlling temperature. Simultaneously, a negative correlation between HCs and DFGCs yields was also observed from Fig. 4a. This phenomenon might indicate that there was an interaction effect on both HCs and DFGCs with evolution of temperature. In fact, the

interplay between biomass-derived oxygenates and plastic-derived hydrocarbons had been widely confirmed by large researches [7, 13, 19, 20, 43]. Besides, DFGCs typically represented the instability of oil, which was a seriously threat to oil store at room temperature [44]. Thus, lowering DFGCs content in oil was necessary considering the future application of oil as an alternative fuel for diesel and jet fuel. Apart from HCs and DFGCs, the other oxygenates mainly comprised ketones, phenols, and esters (Fig. 4a). This result was consistent with that from Chen et al. [11], and Cao et al. [18]. Phenols mainly originated from decomposition of lignin structure [45, 46]. Major ketones was derived from dehydration, degradation, isomerization etc. of cellulose and hemicellulose [34, 47], and the rest of them was derived from the cracking of lignin monomers [48]. Esters were mainly produced by esterification of organic acids with alcohols [49]. Above oxygenates including phenols, esters, and ethers showed an irregular variation trend. This was reasonable considering the complexities of interactions between many hundreds of intermediates from scMeOH co-liquefaction of RS and LLDPE, e.g., radical oxidation of LLDPE in presence of RS to form ketones [20], and interplay between alcohols and ketones [50].

Fig. 4b presents the effect of time on oil chemical compositions at 300 °C. HCs yield in oil with 29.81%, 59.77%, 75.79%, 70.90%, and 62.57% were obtained for 0, 0.5, 1, 1.5, and 2 h, respectively, which were greater than 59% except for 0 h. Apparently, at this temperature, HCs formed quickly within 0.5 h, and its formation was further maximized as time prolonged to 1 h. This result indicates that the initial holding time (i.e., 0.5 h) was crucial factor for HCs formation. After this time, compared to HCs yield maximum (i.e.,

75.79%), it was decreased by 4.89%, and 13.22% for 1.5 and 2 h, respectively. In general, there was an entirely high HCs yield for all holding time, and a low degree change on HCs yield with an exception of 0 h. This result also indicates that time had a limited influence on oil quality. Similar to temperature, an opposite pattern for yields of DFGCs and HCs was also observed in different time. This phenomenon confirmed again that there was a mutual transformation between HCs and DFGCs under evolution of conditions including temperature and time. Apart from DFGCs, similar to irregular changes of other oxygenates e.g., esters, and ethers were observed in different time (Fig. 4b). However, the effect degree of time on these oxygenates contents was noticeably weakened compared to temperature, clearly indicating that temperature played a dominant role in controlling quality of oil. In general, compared with single RS liquefaction (0% of Chen et al. [11], and 10.64% of Cao et al. [18]), the HCs yield from scMeOH liquefaction of RS and LLDPE in present work was significantly higher (75.79% at 300 °C for 1 h, and 70.91% at 300 °C for 1.5 h). It indicates co-thermal conversion of RS with LLDPE in scMeOH was a viable way to produce high-grade oils without catalyst.

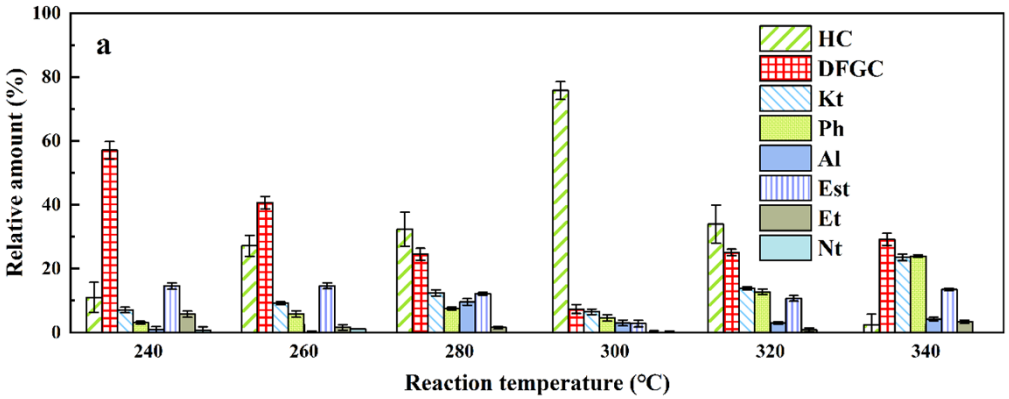

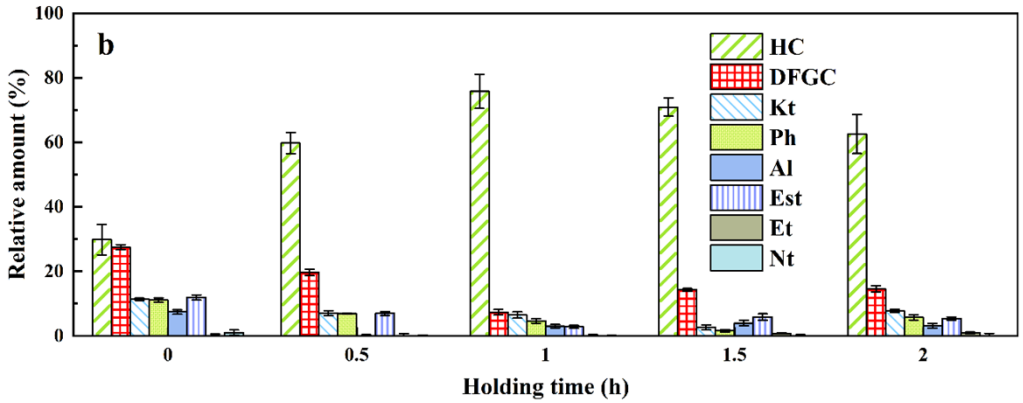

Fig. 4. Chemical compounds grouped distributions of oils from a) varying reaction temperature (i.e., 240 ~ 340 °C) for 1 h and b) holding time (i.e., 0 ~ 2 h) at 300 °C. (HC-Hydrocarbon, DFGC-Diverse functional group compound, Kt-ketone, Ph-Phenol, Al-alcohol, Est-Ester, Et-Ether, Nt-Nitrogen compound). It is noted that DFGCs and other compounds containing oxygen, e.g., Ests, and Als, except for Nts, were all belonged to oxygenated compounds. DFGCs contained more than one functional group and others contained just one functional group.

Fig. 5 summarizes carbon number distributions (CNDs) of all compounds e.g., HCs, DFGCs, esters, and alcohols in oils. For CNDs of oils produced under varying temperature, CNDs of oxygenates mainly distributed in low carbon number range of C_4 ~ C_{10}, while that of HCs spread in a wide carbon number range of C_{11} ~ C_{25}. Below 300 °C, oxygenates preferred low carbon number, i.e., mainly distributing between C_5 ~ C_7. At 300 °C, carbon number of oxygenates shifted towards high carbon number range, i.e., C_8 ~ C_{10} and their content was sharply decreased. Above 300 °C, oxygenates formation were synergistically promoted with moving to higher carbon number (C_7 ~ C_9), indicating the enhancement of interactions between RS and LLDPE or intermediates. Within 0.5 h, the holding time noticeably affected CNDs. After this duration, the holding time showed a weakened effect on CNDs. In general, CNDs of HCs mainly ranged at C_{11} ~ C_{19}, and only a few amounts of long chain HCs, e.g., heneicosane ($C_{21}H_{44}$), and 2-methyltetracosane ($C_{25}H_{52}$), existed in compounds, implying that oils produced under 300 °C for 0.5, 1, 1.5, and 2 h were all attractive as gasoline or jet fuel with further upgrading. All these results

show that scMeOH co-liquefaction of RS and LLDPE was an efficient way to produce high-grade oil free of catalyst.

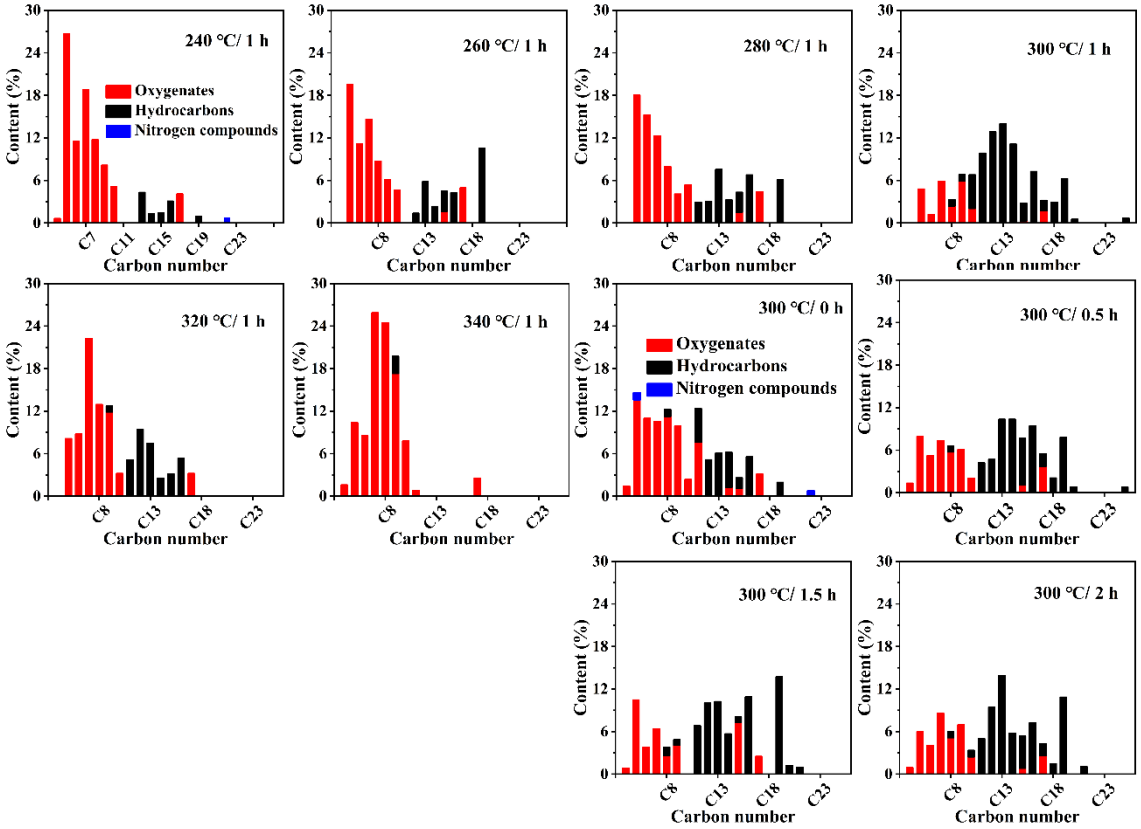

Fig. 5. Effects of temperature and time on carbon number distribution of compounds, e.g., hydrocarbons, esters, and alcohols, in oils. a, temperature. b, time.

3.3 Effects of temperature and time on solid products properties

Fig. 6a and b show the elemental analysis and higher heating value (HHV) (by Eq. 6) of solid products from different temperature (i.e., 240 ~ 340 °C) for 1 h, and at 300 °C for various time (i.e., 0 ~ 2 h), respectively. As seen in Fig. 6a, oxygen content was decreased sharply from 30.26 wt% to 1.71 wt% when temperature was increased from 240 °C to 260 °C. This indicates that RS was dramatically degraded at 260 °C. It could be confirmed by the following indications. First, an obvious carbonization phenomenon for solid products from 240 °C and 260 °C shows that RS/LLDPE mixture began to degrade noticeably at 260 °C (Fig. 6c). Second, the evolution of functional groups

compositions of solid product at 240 °C was similar to those of RS. The absorbance peaks between 3200 and 3380 cm^{-1} was ascribed to O-H stretching vibrations, representing organic compounds containing functional group of -OH (e.g., reformed cellulose, and hemicellulose), and this peak almost disappeared at 260 °C, showing the noticeable degradation of RS (Fig. 6d). For solid products obtained under temperature of 280 °C~340 °C, no obvious difference was observed in oxygen content. The carbon and hydrogen content also remained stable within the range of 79.59 ~ 81.26% and 12.18 ~ 13.97%, respectively. Besides, high HHV (43.96 ~ 47.23 MJ/kg) of solid products was obtained under temperature of 260~340 °C, implying that these solid products could be used as alternative solid fuel. Regarding solid products from different time, a little difference in element content and HHV (45.21 ~ 47.00 MJ/kg) was observed (Fig. 6b). Additionally, Fig. 6e also depicts that the holding time had little influence on functional groups compositions. According to all these results, it could be concluded that the holding time had a limited effect on products distribution, chemical compositions of oils, elemental compositions and functional group characteristics of solid products at 300 °C.

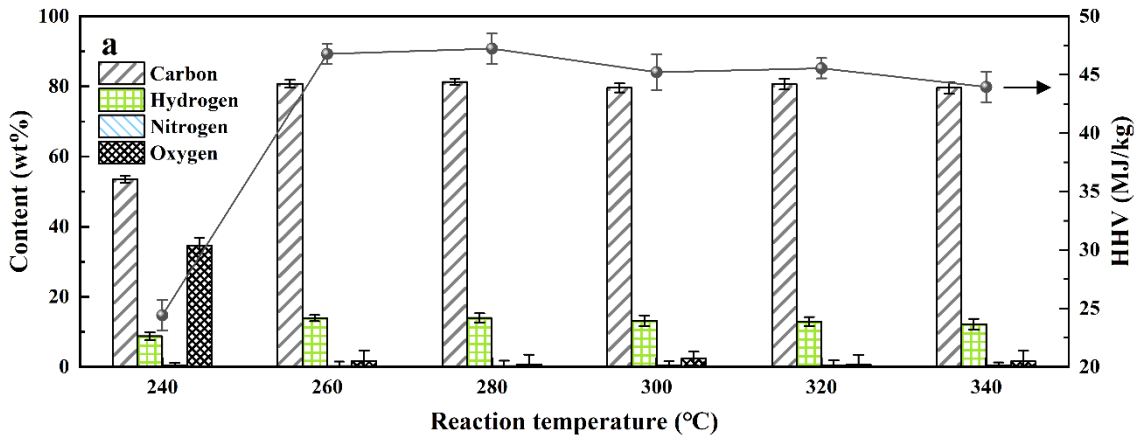

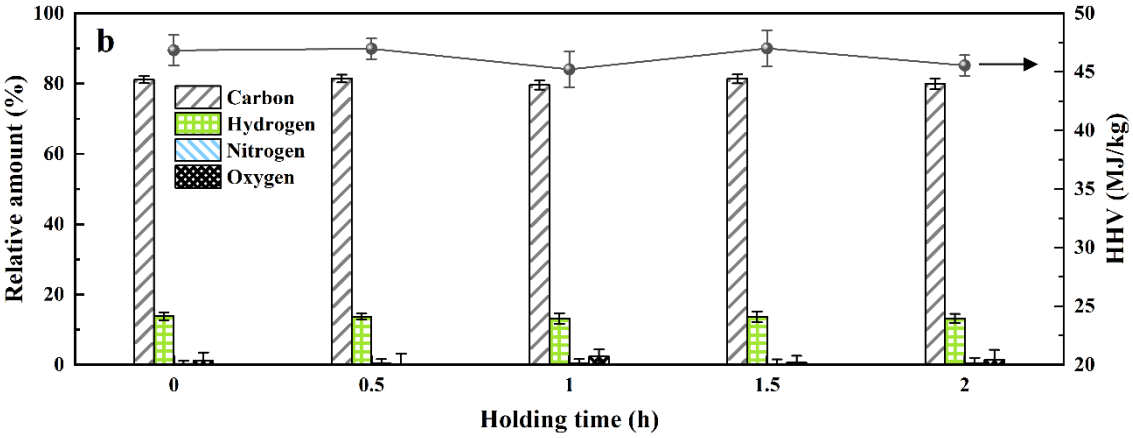
b
Carbon
Hydrogen
Nitrogen
Oxygen
Relative amount (%)
HHV (MJ/kg)
Holding time (h)
0
0.5
1
1.5
2

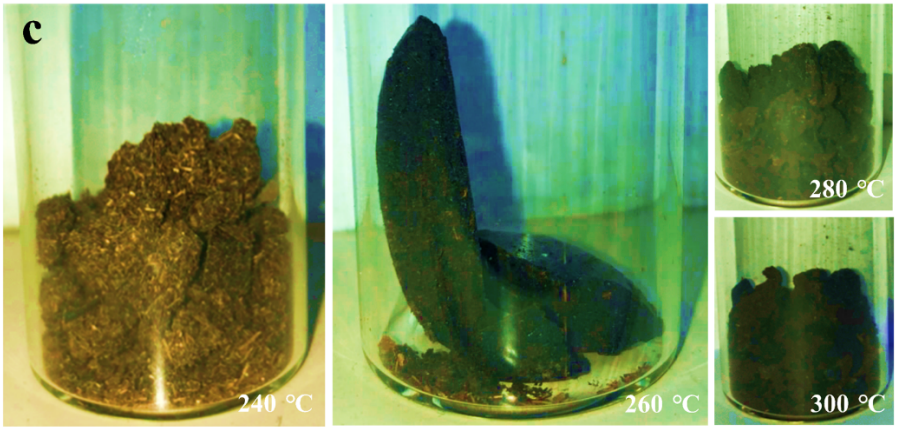
c
240 °C
260 °C
280 °C
300 °C

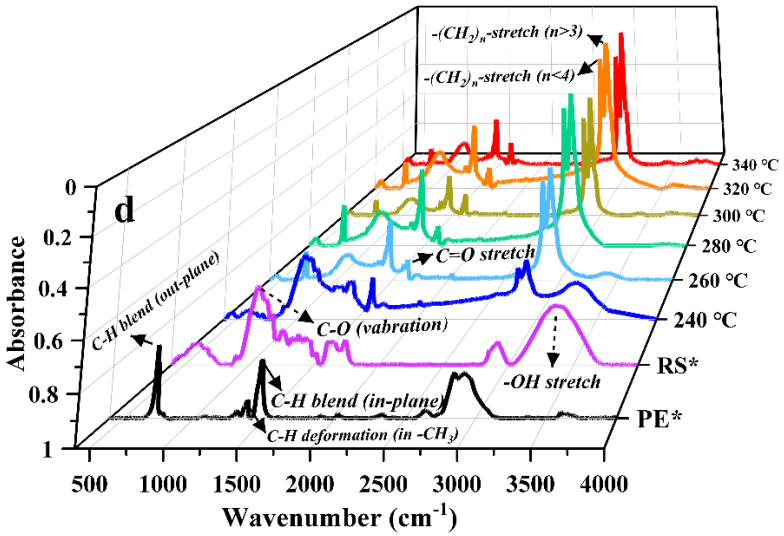
d
-(CH2)n-stretch (n>3)
-(CH2)n-stretch (n<4)
C=O stretch
C-O (vabration)
C-H blend (out-plane)
C-H blend (in-plane)
C-H deformation (in -CH3)
-OH stretch
340 °C
320 °C
300 °C
280 °C
260 °C
240 °C
RS*
PE*
Absorbance
Wavenumber (cm-1)

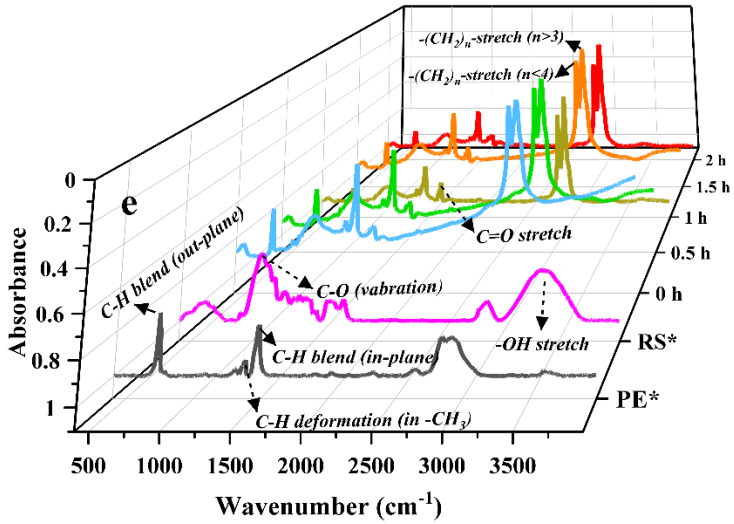

Fig. 6. Fundamental data of solid products obtained from various conditions. a), and b), EA of solid products (carbon, hydrogen, oxygen, nitrogen, and HHV) obtained varying reaction temperature (i.e., 240 ~ 340 °C) for 1 h, and different holing time (i.e., 0 ~ 2 h) at 300 °C. c), variation of solid products shape obtained from 240, 260, 280, and 300 °C. d), and e), FT-IR spectra of feedstocks, and solid products between 500 ~ 4000 cm $^{-1}$ obtained from various conditions.

Fig. 7a compares the TG curves of solid products generated under various temperature for 1 h, and those of both feedstocks were also listed for a comparison. A similar degradation trend was observed for RS and solid product from 240 °C, further evidencing that a few amounts of RS were decomposed at 240 °C. For solid products derived from scMeOH co-liquefaction at 260 ~ 340 °C, their initial decomposition temperature continuously moved towards low temperatures. It implies that the thermal stability of solid products was reduced with an increase of reaction temperature, and more LLDPE was converted into gas and oil products. Regarding influence of time, there was a little difference in thermal stability between solid products at 300 °C for various time (i.e., 0 ~ 2 h) (Fig. 7b). This result indicates that the holding time had a limited influence on synergistic degradation of LLDPE towards oil or gas during co-liquefying with RS.

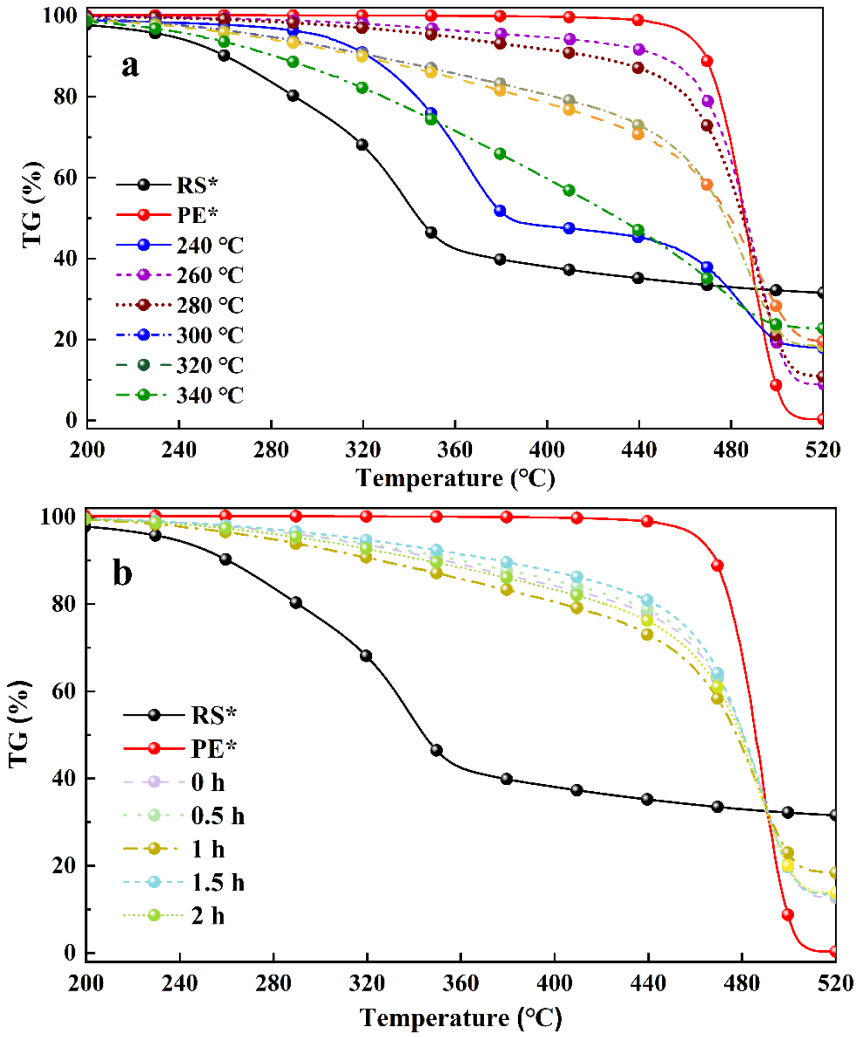

Fig. 7. TG curves of solid products obtained from a) various temperature (i.e., 240 ~ 340 °C) for 1 h, and b) different time (i.e., 0 ~ 2 h) at 300 °C.

SEM was presented in Fig. 8 to further investigate the other possible potential utilization of solid products containing micro plastic. A nearly complete fiber structure was observed for solid product obtained at 240 °C, indicating few RS was degraded under this temperature. After this temperature, the surface of all solid products shifted towards smooth, and there was no obvious difference in images of solid products. These results directly strong confirm that RS was significantly degraded after 240 °C. Simultaneously, a smooth surface of solid products was observed for all time (0~2 h). This phenomenon was mainly attributed to the melting and reforming of LLDPE in solid product. Therefore, it could conclude that the solid products obtained from scMeOH co-liquefaction of RS

and LLDPE could not be used as soil amendment due to potential micro plastic. Besides, all solid products presented a smooth surface without pores, indicating that solid products could not used as materials needing pores, e.g., catalyst, and adsorbent.

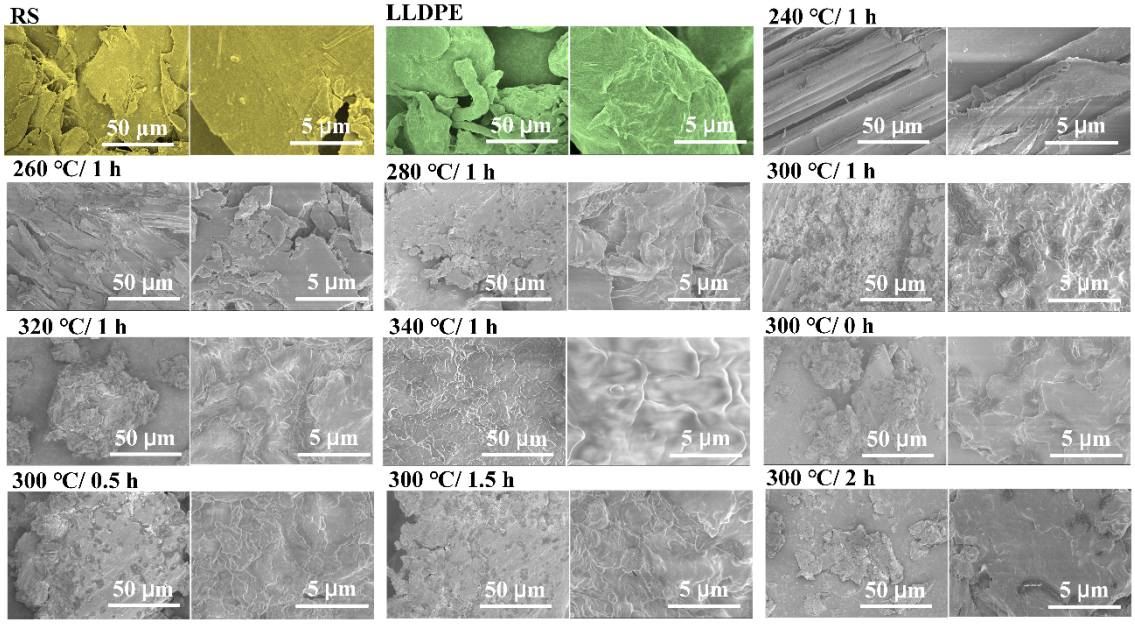

Fig. 8. SEM of feedstocks and solid products under various conditions.

3.4 Limitations and prospects

Although the present study had comprehensively explored the effects of reaction temperature and holding time on yields and properties of liquefaction products, there were still some limitations those we need to focus and overcome in the future. Firstly, this work produced a significant amount of solid products. It is necessary to find tome feasible way to realize its value-added utilization. Here, we presented the scMeOH co-liquefaction of RS and LLDPE at higher temperature of 400 °C for 1 h to further degrade the remaining solid residue. The results of products yield and properties were presented in Fig. S1. As presented, although the yield of solid products was reduced to 16.44 wt% (Fig. S1a), the HCs content in oil was only 21.54% (Fig. S1b), only accounting for 28.42% and 30.38% of that obtained at 300 °C for 1 h and 1.5 h, respectively. The disappeared peak of -OH

stretch at 3403 cm^{-1} and weakened peak of C-O vibration at 1053 cm^{-1} (Fig. S1c) confirmed that RS derived free radicals containing oxygen reacted with oligomers ($C_{x-m}H_{y-n}$•) from LLDPE, resulting in low HCs yield. Besides, low degradation temperature of 112.19 °C for solid product showed that LLDPE had been significantly decomposed under 400 °C (Fig. S1d). This indicates that large free radicals of hydrocarbons ($C_{x-m}H_{y-n}$•) derived from LLDPE would directly involve in reaction. The results show that the synergistic effect at 400 °C was beneficial for further degradation solid product into light molecular compounds rather than producing HCs-rich oil. Thus, the potential utilization of solid residue should be considered as other directions, such as organic amendment and asphalt.

Secondly, the role of methanol during reaction was unclear. Previous studies could be summarized as two aspects as follows. First, large amount of methanol involved reactions in the presence of catalyst [51, 52]. Second, methanol did not react in the absence of catalyst [37]. However, many researchers had stated that the media simultaneously played two roles of solvent and reactant in liquefaction process without catalyst. Pei et al. [53] observed many oxygenated compounds for single HDPE-derived oil from supercritical ethanol co-liquefaction of microalgae and HDPE without catalyst, which strongly evidenced that ethanol involved the liquefaction process. Unfortunately, this work did not talk much about the ethanol consumption.

Finally, more attention should be paid on the sustainability features of scMeOH co-liquefaction of LCB and plastic, which should be investigated by employing the advanced sustainability assessment tools, e.g., life cycle assessment, exergy and its combinations

with environmental and economic parameters. Aghbashlo et al [54] had looked into the application of these techniques in assessing the sustainability features of bioenergy production systems. Chen et al. [55] also successfully evaluated the hydrothermal liquefaction microalgae by open-source techno-economic analysis and life cycle assessment. These technique should be also introduced to evaluate the utilization of supercritical technique to recycle wastes.

4. Conclusions

scMeOH co-liquefaction of RS and LLDPE were studied in the temperature range of 240 ~ 340 °C for 0 ~2 h. Some conclusions could be summarized as follows:

1) the reaction temperature but not the holding time dominated the oil and solid product yields, chemical compositions of oils, elemental compositions, thermal stability, etc. of solid products. Higher temperature resulted in more LLDPE to degrade, resulting in higher oil production but not higher hydrocarbons content in oil.

2) Among all conditions tested, 30.07 wt% of oil yield with 75.79% of hydrocarbons content and 33.05 wt% oil yield with 70.91% hydrocarbon content were obtained under 300 °C for 1 h and 1.5 h, respectively, which were determined as optimum parameters to produce high-grade oil. Under these conditions, as high as 53.85 wt% and 48.28 wt% yields of solid products were also obtained.

3) Solid products could be applied as sustainable carbon resources because of high carbon content (79.59% ~ 81.26%), and solid fuel due to high HHV (43.96 MJ/kg ~ 47.23 MJ/kg). However, they could not be utilized as soil amendment resulting from their potential micro plastic pollution, and materials (catalyst, adsorbent, etc.) needing pore

structure due to the smooth surface without pores.

Declaration of competing interest

There are no conflicts to declare.

Acknowledgments

This work was supported by the Graduate Research & Practice Innovation Program of Jiangsu Province (SJCX21_1003), the National Natural Science Foundation of China (Grant No.51706240, No.52076125), and the China Scholarship Council ([2018]5046, International Clean Energy Talent Program 2018).

Supporting information

Distribution and properties of products obtained from high reaction condition of 400 °C for 1 h. a) products distribution. b) chemical compositions of oil. c) FT-IR of solid product. d) TGA of solid product (PE = LLDPE) (Fig. S1), Highlights and limitations from main works about liquefying RS by the present study and other authors (Table S1), Data for GC-MS result of oils derived from various reaction temperature (Table S2), and Data for GC-MS result of oils derived from various holding time (Table S3).

References

[1] X.-S. Zhang, G.-X. Yang, H. Jiang, W.-J. Liu, H.-S. Ding, Mass production of chemicals from biomass-derived oil by directly atmospheric distillation coupled with co-pyrolysis, Scientific Reports, 3 (2013) 1120. https://doi.org/10.1038/srep01120

[2] H. Kazemi Shariat Panahi, M. Dehhaghi, J.E. Kinder, T.C. Ezeji, A review on green liquid fuels for the transportation sector: a prospect of microbial solutions to climate change, Biofuel Research Journal, 6 (2019) 995-1024. https://doi.org/10.18331/brj2019.6.3.2

[3] L. Leng, W. Li, H. Li, S. Jiang, W. Zhou, Cold Flow Properties of Biodiesel and the Improvement Methods: A Review, Energy & Fuels, 34 (2020) 10364-10383.

https://doi.org/10.1021/acs.energyfuels.0c01912

[4] S.M.H.D. Perera, C. Wickramasinghe, B.K.T. Samarasiri, M. Narayana, Modeling of thermochemical conversion of waste biomass – a comprehensive review, Biofuel Research Journal, 8 (2021) 1481-1528. https://doi.org/10.18331/BRJ2021.8.4.3

[5] M.K. Jindal, M.K. Jha, Effect of process parameters on hydrothermal liquefaction of waste furniture sawdust for bio-oil production, RSC Advances, 6 (2016) 41772-41780. https://doi.org/10.1039/c6ra02868c

[6] J. Arun, K.P. Gopinath, P. SundarRajan, M. JoselynMonica, V. Felix, Co-liquefaction of Prosopis juliflora with polyolefin waste for production of high grade liquid hydrocarbons, Bioresource technology, 274 (2019) 296-301. https://doi.org/10.1016/j.biortech.2018.11.102

[7] X. Wu, J. Liang, Y. Wu, H. Hu, S. Huang, K. Wu, Co-liquefaction of microalgae and polypropylene in sub-/super-critical water, RSC Advances, 7 (2017) 13768-13776. https://doi.org/10.1039/c7ra01030c

[8] R. Singh, K. Chaudhary, B. Biswas, B. Balagurumurthy, T. Bhaskar, Hydrothermal liquefaction of rice straw: Effect of reaction environment, The Journal of Supercritical Fluids, 104 (2015) 70-75. https://doi.org/https://doi.org/10.1016/j.supflu.2015.05.027

[9] X. Zhu, W. Qian, X. Li, S. Tong, Z. Hu, Y. Huang, A. Xia, H. Yao, Moisture adsorption and spontaneous combustion characteristics of biomass wastes after degradative solvent extraction, Fuel, 266 (2020) 117109. https://doi.org/https://doi.org/10.1016/j.fuel.2020.117109

[10] R. Younas, S. Hao, L. Zhang, S. Zhang, Hydrothermal liquefaction of rice straw with NiO nanocatalyst for bio-oil production, Renewable Energy, 113 (2017) 532-545. https://doi.org/10.1016/j.renene.2017.06.032

[11] D. Chen, Q. Ma, L. Wei, N. Li, Q. Shen, W. Tian, J. Zhou, J. Long, Catalytic hydroliquefaction of rice straw for bio-oil production using Ni/CeO 2 catalysts, Journal of Analytical and Applied Pyrolysis, 130 (2018) 169-180. https://doi.org/10.1016/j.jaap.2018.01.012

[12] D.K. Ojha, R. Vinu, Fast co-pyrolysis of cellulose and polypropylene using Py-GC/MS and Py-FT-IR, RSC Advances, 5 (2015) 66861-66870. https://doi.org/10.1039/c5ra10820a

[13] J. Yang, Q. He, L. Yang, A review on hydrothermal co-liquefaction of biomass, Applied Energy, 250 (2019) 926-945.

https://doi.org/https://doi.org/10.1016/j.apenergy.2019.05.033

[14] H.-J. Huang, Y.-C. Chang, F.-Y. Lai, C.-F. Zhou, Z.-Q. Pan, X.-F. Xiao, J.-X. Wang, C.-H. Zhou, Co-liquefaction of sewage sludge and rice straw/wood sawdust: The effect of process parameters on the yields/properties of bio-oil and biochar products, Energy, 173 (2019) 140-150. https://doi.org/10.1016/j.energy.2019.02.071

[15] P. Lu, Q. Huang, A.C. Bourtsalas, Y. Chi, J. Yan, Synergistic effects on char and oil produced by the co-pyrolysis of pine wood, polyethylene and polyvinyl chloride, Fuel, 230 (2018) 359-367. https://doi.org/10.1016/j.fuel.2018.05.072

[16] X. Yuan, H. Li, G. Zeng, J. Tong, W. Xie, Sub- and supercritical liquefaction of rice straw in the presence of ethanol–water and 2-propanol–water mixture, Energy, 32 (2007) 2081-2088. https://doi.org/10.1016/j.energy.2007.04.011

[17] H. Li, X. Yuan, G. Zeng, J. Tong, Y. Yan, H. Cao, L. Wang, M. Cheng, J. Zhang, D. Yang, Liquefaction of rice straw in sub- and supercritical 1,4-dioxane–water mixture, Fuel Processing Technology, 90 (2009) 657-663. https://doi.org/10.1016/j.fuproc.2008.12.003

[18] L. Cao, C. Zhang, S. Hao, G. Luo, S. Zhang, J. Chen, Effect of glycerol as co-solvent on yields of bio-oil from rice straw through hydrothermal liquefaction, Bioresource technology, 220 (2016) 471-478. https://doi.org/10.1016/j.biortech.2016.08.110

[19] J. Souza dos Passos, M. Glasius, P. Biller, Hydrothermal Co-Liquefaction of Synthetic Polymers and Miscanthus giganteus: Synergistic and Antagonistic Effects, ACS Sustainable Chemistry & Engineering, 8 (2020) 19051-19061. https://doi.org/10.1021/acssuschemeng.0c07317

[20] S. Raikova, T.D.J. Knowles, M.J. Allen, C.J. Chuck, Co-liquefaction of Macroalgae with Common Marine Plastic Pollutants, ACS Sustainable Chemistry & Engineering, 7 (2019) 6769-6781. https://doi.org/10.1021/acssuschemeng.8b06031

[21] S. Hongthong, S. Raikova, H.S. Leese, C.J. Chuck, Co-processing of common plastics with pistachio hulls via hydrothermal liquefaction, Waste Management, 102 (2020) 351-361. https://doi.org/https://doi.org/10.1016/j.wasman.2019.11.003

[22] S. Hongthong, H.S. Leese, C.J. Chuck, Valorizing Plastic-Contaminated Waste Streams through the Catalytic Hydrothermal Processing of Polypropylene with Lignocellulose, ACS Omega, 5 (2020) 20586-20598.

https://doi.org/10.1021/acsomega.0c02854

[23] P. Zhao, Z. Yuan, X. Song, J. Zhang, A.J. Ragauskas, Product Characteristics and Synergy Study on Supercritical Methanol Liquefaction of Lignocellulosic Biomass and Plastic, ACS Sustainable Chemistry & Engineering, 9 (2021) 17103-17111. https://doi.org/10.1021/acssuschemeng.1c04289

[24] L. Hadhoum, G. Burnens, K. Loubar, M. Balistrou, M. Tazerout, Bio-oil recovery from olive mill wastewater in sub-/supercritical alcohol-water system, Fuel, 252 (2019) 360-370. https://doi.org/https://doi.org/10.1016/j.fuel.2019.04.133

[25] B. Zhao, H. Wang, Y. Hu, J. Gao, G. Zhao, M.B. Ray, C.C. Xu, Hydrothermal Co-Liquefaction of Lignite and Lignocellulosic Biomass with the Addition of Formic Acid: Study on Product Distribution, Characteristics, and Synergistic Effects, Industrial & Engineering Chemistry Research, 59 (2020) 21663-21675. https://doi.org/10.1021/acs.iecr.0c04619

[26] X. Chen, X. Peng, X. Ma, J. Wang, Investigation of Mannich reaction during co-liquefaction of microalgae and sweet potato waste, Bioresource technology, 284 (2019) 286-292. https://doi.org/https://doi.org/10.1016/j.biortech.2019.03.136

[27] W.T. Chen, Y. Zhang, J. Zhang, G. Yu, L.C. Schideman, P. Zhang, M. Minarick, Hydrothermal liquefaction of mixed-culture algal biomass from wastewater treatment system into bio-crude oil, Bioresource technology, 152 (2014) 130-139. https://doi.org/10.1016/j.biortech.2013.10.111

[28] W. Chen, K. Jin, N. Linda Wang, Use of Supercritical Water for the Liquefaction of Polypropylene into Oil, ACS Sustainable Chemistry & Engineering, 7 (2019) 3749-3758. https://doi.org/10.1021/acssuschemeng.8b03841

[29] J. Li, Y. Lai, X. Zhu, Q. Liao, A. Xia, Y. Huang, X. Zhu, Pyrolysis kinetics and reaction mechanism of the electrode materials during the spent LiCoO2 batteries recovery process, Journal of Hazardous Materials, 398 (2020) 122955. https://doi.org/https://doi.org/10.1016/j.jhazmat.2020.122955

[30] L. Baskoro, A. Muhammad, K. Yoshikawa, F. Takahashi, Energy and resource recovery from Tetra Pak waste using hydrothermal treatment, Applied Energy, 207 (2017) 107-113. https://doi.org/10.1016/j.apenergy.2017.05.141

[31] Y. Wang, Y. Wang, Y. Zhu, C. Fang, D. Xu, X. Zheng, Interactions of the Main Components in Paper-Plastic-Aluminum Complex Packaging Wastes during the Hydrothermal Liquefaction Process, Chemical Engineering & Technology, 44 (2021) 1519-1527. https://doi.org/10.1002/ceat.202100124

[32] J. Xu, X. Xie, J. Wang, J. Jiang, Directional liquefaction coupling fractionation of lignocellulosic biomass for platform chemicals, Green Chemistry, 18 (2016) 3124-3138. https://doi.org/10.1039/C5GC03070F

[33] J. Yang, Q. He, H. Niu, K. Corscadden, T. Astatkie, Hydrothermal liquefaction of biomass model components for product yield prediction and reaction pathways exploration, Applied Energy, 228 (2018) 1618-1628. https://doi.org/https://doi.org/10.1016/j.apenergy.2018.06.142

[34] H.-j. Huang, X.-z. Yuan, Recent progress in the direct liquefaction of typical biomass, Progress in Energy and Combustion Science, 49 (2015) 59-80. https://doi.org/https://doi.org/10.1016/j.pecs.2015.01.003

[35] R. Singh, V. Srivastava, K. Chaudhary, P. Gupta, A. Prakash, B. Balagurumurthy, T. Bhaskar, Conversion of rice straw to monomeric phenols under supercritical methanol and ethanol, Bioresource technology, 188 (2015) 280-286. https://doi.org/10.1016/j.biortech.2015.01.001

[36] H.A. Baloch, S. Nizamuddin, M.T.H. Siddiqui, N.M. Mubarak, S. Mazari, G.J. Griffin, M.P. Srinivasan, Co-liquefaction of synthetic polyethylene and polyethylene bags with sugarcane bagasse under supercritical conditions: A comparative study, Renewable Energy, 162 (2020) 2397-2407. https://doi.org/10.1016/j.renene.2020.10.008

[37] X. Wang, X.-A. Xie, J. Sun, W. Liao, Effects of liquefaction parameters of cellulose in supercritical solvents of methanol, ethanol and acetone on products yield and compositions, Bioresource technology, 275 (2019) 123-129. https://doi.org/10.1016/j.biortech.2018.12.047

[38] H. Prajitno, J. Park, C. Ryu, H.Y. Park, H.S. Lim, J. Kim, Effects of solvent participation and controlled product separation on biomass liquefaction: A case study of sewage sludge, Applied Energy, 218 (2018) 402-416. https://doi.org/https://doi.org/10.1016/j.apenergy.2018.03.008

[39] Z. Wang, K.G. Burra, T. Lei, A.K. Gupta, Co-pyrolysis of waste plastic and solid biomass for synergistic production of biofuels and chemicals-A review, Progress in Energy and Combustion Science, 84 (2021) 100899. https://doi.org/https://doi.org/10.1016/j.pecs.2020.100899

[40] Z. He, B. Wang, B. Zhang, H. Feng, S. Kandasamy, H. Chen, Synergistic effect of hydrothermal Co-liquefaction of Spirulina platensis and Lignin: Optimization of operating parameters by response surface methodology, Energy, 201 (2020) 117550. https://doi.org/10.1016/j.energy.2020.117550

[41] H. Chen, Z. He, B. Zhang, H. Feng, S. Kandasamy, B. Wang, Effects of the aqueous phase recycling on bio-oil yield in hydrothermal liquefaction of Spirulina Platensis, α-cellulose, and lignin, Energy, 179 (2019) 1103-1113. https://doi.org/https://doi.org/10.1016/j.energy.2019.04.184

[42] M.S. Seshasayee, P.E. Savage, Synergistic interactions during hydrothermal liquefaction of plastics and biomolecules, Chemical Engineering Journal, 417 (2021) 129268. https://doi.org/https://doi.org/10.1016/j.cej.2021.129268

[43] X. Yuan, H. Cao, H. Li, G. Zeng, J. Tong, L. Wang, Quantitative and qualitative analysis of products formed during co-liquefaction of biomass and synthetic polymer mixtures in sub- and supercritical water, Fuel Processing Technology, 90 (2009) 428-434. https://doi.org/10.1016/j.fuproc.2008.11.005

[44] A. Demirbas, Competitive liquid biofuels from biomass, Applied Energy, 88 (2011) 17-28. https://doi.org/https://doi.org/10.1016/j.apenergy.2010.07.016

[45] Z. Ye, S. Xiu, A. Shahbazi, S. Zhu, Co-liquefaction of swine manure and crude glycerol to bio-oil: Model compound studies and reaction pathways, Bioresource technology, 104 (2012) 783-787. https://doi.org/10.1016/j.biortech.2011.09.126

[46] S. Kang, X. Li, J. Fan, J. Chang, Hydrothermal conversion of lignin: A review, Renewable and Sustainable Energy Reviews, 27 (2013) 546-558. https://doi.org/10.1016/j.rser.2013.07.013

[47] H.-x. Tao, X.-a. Xie, C.-z. Tang, W.-g. Tian, Mechanism of ketones formation from cellulose liquefaction in sub- and supercritical ethanol, Journal of Fuel Chemistry and Technology, 41 (2013) 60-66. https://doi.org/10.1016/s1872-5813(13)60010-9

[48] H.A. Baloch, M.T.H. Siddiqui, S. Nizamuddin, S. Riaz, M. Haris, N.M. Mubarak, G.J. Griffin, M.P. Srinivasan, Effect of solvent on hydro-solvothermal co liquefaction of sugarcane bagasse and polyethylene for bio-oil production in ethanol–water system, Process Safety and Environmental Protection, 148 (2021) 1060-1069. https://doi.org/https://doi.org/10.1016/j.psep.2021.02.015

[49] H.-j. Huang, X.-z. Yuan, B.-t. Li, Y.-d. Xiao, G.-m. Zeng, Thermochemical liquefaction characteristics of sewage sludge in different organic solvents, Journal of Analytical and Applied Pyrolysis, 109 (2014) 176-184. https://doi.org/https://doi.org/10.1016/j.jaap.2014.06.015

[50] T. Moriya, H. Enomoto, Characteristics of polyethylene cracking in supercritical water compared to thermal cracking, Polymer Degradation and Stability, 65 (1999) 373-386. https://doi.org/https://doi.org/10.1016/S0141-3910(99)00026-9

[51] P.H. Galebach, D.J. McClelland, N.M. Eagan, A.M. Wittrig, J.S. Buchanan, J.A. Dumesic, G.W. Huber, Production of Alcohols from Cellulose by Supercritical Methanol Depolymerization and Hydrodeoxygenation, ACS Sustainable Chemistry & Engineering, 6 (2018) 4330-4344. https://doi.org/10.1021/acssuschemeng.7b04820

[52] S. Cheng, L. Wei, J. Julson, K. Muthukumarappan, P.R. Kharel, Upgrading pyrolysis bio-oil to biofuel over bifunctional Co-Zn/HZSM-5 catalyst in supercritical methanol, Energy Conversion and Management, 147 (2017) 19-28. https://doi.org/10.1016/j.enconman.2017.05.044

[53] X. Pei, X. Yuan, G. Zeng, H. Huang, J. Wang, H. Li, H. Zhu, Co-liquefaction of microalgae and synthetic polymer mixture in sub- and supercritical ethanol, Fuel Processing Technology, 93 (2012) 35-44. https://doi.org/10.1016/j.fuproc.2011.09.010

[54] M. Aghbashlo, Z. Khounani, H. Hosseinzadeh-Bandbafha, V.K. Gupta, H. Amiri, S.S. Lam, T. Morosuk, M. Tabatabaei, Exergoenvironmental analysis of bioenergy systems: A comprehensive review, Renewable and Sustainable Energy Reviews, 149 (2021) 111399. https://doi.org/https://doi.org/10.1016/j.rser.2021.111399

[55] P.H. Chen, J.C. Quinn, Microalgae to biofuels through hydrothermal liquefaction: Open-source techno-economic analysis and life cycle assessment, Applied Energy, 289 (2021) 116613. https://doi.org/10.1016/j.apenergy.2021.116613